Global and Planetary Change 215 (2022) 103868

Contents lists available at ScienceDirect

Global and Planetary Change

journal homepage: www.elsevier.com/locate/gloplacha

Analysis of soil moisture trends in Europe using rank-based and empirical decomposition approaches

Laura Almendra-Martín [a,*], José Martínez-Fernández [a], María Piles [b], Ángel González-Zamora [a], Pilar Benito-Verdugo [a], Jaime Gaona [a]

[a] Instituto de Investigación en Agrobiotecnología, CIALE, Universidad de Salamanca, Villamayor, 37185 Salamanca, Spain
[b] Image Processing Laboratory, Universitat de València, 46980 València, Spain

ARTICLE INFO

Editor: Dr Jed O Kaplan

Keywords:
Soil moisture
Trends
Drought
Duration
Intensity
Onset
Mann-Kendall
Empirical Mode Decomposition

ABSTRACT

The impact of climate change on soil moisture (SM) dynamics is uncertain. Changes in the Earth's SM during recent decades have been studied globally and in different regions, but little attention has been given to Europe. In addition, most previous works have just relied on a monotonic behavior of SM changes, which is a strong assumption and not always valid. We argue that this fact, together with the use of large temporal scales, has prevented the observation of clear patterns of SM trends over the continent. In this work, we study European SM trends for a 30-year period, from 1991 to 2020, using two complementary databases, one from reanalysis project ERA5-Land and the other from the model Lisflood. Both rank-based and empirical decomposition approaches have been considered and applied to monthly and annual series of SM anomalies. The Köppen-Geiger classification allowed us to analyze the distribution of SM anomaly trends in the separate European climates. The results obtained with both databases, methods and temporal scales were consistent, with the empirical decomposition method generally detecting more significant trends. Our results show a general decreasing trend of SM, regardless of climate type but more intense in Eastern and Central Europe. In addition, the rank-based method detected fewer positive trends, suggesting a non-monotonic behavior in changes to wetter conditions. The most notable differences were obtained with the empirical decomposition method when comparing the different temporal scales. Hence, an intramonthly analysis was conducted to provide insight into the different patterns. An increase in significant trends was observed in April and the autumn (September–October-November). Furthermore, we conducted a similar analysis to study trends in extreme drought characteristics (annual duration, intensity and onset) and we obtained consistent results, with the empirical decomposition method detecting more significant trends. Our investigations show a general increase in the duration and intensity of extreme droughts over the European continent, tending to be delayed a few days per year in arid and temperate regions.

1. Introduction

Soil moisture (SM) is considered an essential climate variable (GCOS, 2010). It exerts control on the water and energy exchange between the soil and the atmosphere, as it behaves as a storage component for precipitation and induces persistence in the climate system (Martínez-Fernández et al., 2021; Piles et al., 2021; Seneviratne et al., 2010). Climate change is predicted to disrupt many environmental and, therefore, social and economic processes (Grillakis, 2019). Subsequently, it is likely that SM dynamics will also be affected and thereby alter the availability of water for plants (Kramer, 1944), the runoff yield (Merz and Plate, 1997) or the intensity and frequency of droughts (Martínez-Fernández et al., 2015). However, the magnitude and extent of these changes are still uncertain (Cheng et al., 2017).

There are several studies dedicated to the study of the SM trend, both on global (Albergel et al., 2013; Dorigo et al., 2012; Feng and Zhang, 2015; Piles et al., 2019; Sheffield and Wood, 2007) and regional scales (An et al., 2016; Li et al., 2015; Qiu et al., 2016; Rahmani et al., 2016; Trnka et al., 2009; Zawadzki and Kędzior, 2014). Most of those studies just analyzed a monotonic trend, but SM, as many hydroclimatic variables, exhibits nonlinear and non-stationary changes (Bai et al., 2015). Additionally, the computed trends are known to strongly depend on the period of study (Hänsel et al., 2019; Sang et al., 2014) and the temporal scale analyzed (Gudmundsson and Seneviratne, 2015; Sang et al., 2021),

* Corresponding author.
E-mail address: lauraalmendra@usal.es (L. Almendra-Martín).

https://doi.org/10.1016/j.gloplacha.2022.103868
Received 30 December 2021; Received in revised form 8 June 2022; Accepted 9 June 2022
Available online 13 June 2022

especially when monotonic approaches are used. Hence, the extended use of methods that just account monotonic behavior to estimate SM changes has led in some cases to discrepancies between trends of series with different time scales or periods, which are difficult to interpret and reconcile (Dai, 2013). In particular, few trends have been observed in Europe when monotonic behavior is assumed (Albergel et al., 2013; Cammalleri et al., 2016; Dorigo et al., 2012; Zawadzki and Kędzior, 2014). In contrast, trends in drought indices, runoff, temperature, precipitation or evaporation have shown statistical significance in this region (Gudmundsson and Seneviratne, 2015; Hänsel et al., 2019; Jaagus et al., 2021; Masseroni et al., 2021; Song et al., 2020; Vautard et al., 2007), which suggests that the existence of similar trends in SM would be expected. Some studies have reported SM changes in recent decades throughout Europe. For example, Cammalleri et al. (2016) found differences between the year-average deficit water in most of the European soil surface. In regional studies, Almendra-Martín et al. (2021a) observed a general decreasing trend of SM in the Iberian Peninsula, and Trnka et al. (2008) analyzed SM derived by precipitation and temperature in situ series in the Czech Republic and found a larger number of climatic stations with significant trends.

Although some studies have analyzed nonlinear trends of hydroclimatic variables (Adarsh and Janga Reddy, 2019; Bordi et al., 2009; Carmona and Poveda, 2014; Wei et al., 2018), only a few are focused on SM series. Deng et al. (2020) found a change in the SM trend at the global scale in 2001 with a changing rate twice that of the previous period. Pan et al. (2019) proposed a nonlinear approach to estimate trends based on a polynomial fit. However, the general best fit they obtained was a first-degree polynomial, namely, a linear approach. Trend identification in hydrologic time series is not a trivial task (Bordi et al., 2009; Sang et al., 2013), and many novel methods have been used to accurately identify components in its series (Sang et al., 2014), but very few of them have accounted for nonlinear SM behavior (Bueso et al., 2020; Cheng and Huang, 2016; Piles et al., 2019).

Unlike other hydroclimatic variables, the study of SM trends has not received special attention until recent years due to a lack of long-term and continuous databases. For the stable records of climate, it is considered that a climatological-length series is needed (Merchant et al., 2014), and few databases of SM have that length. Remote sensing databases, such as the European Space Agency Climate Change Initiative (CCI) SM, provide spatial-temporal continuous series. However, some limitations are found in such databases, such as data gaps (Almendra-Martín et al., 2021b) or breaks due to its merging algorithm (Preimesberger et al., 2020). In contrast, the latest advances in land surface modelling and assimilation of observations in reanalysis ensure the completeness of separate variables at the global scale, such as SM, to enhance research in climate change studies (Muñoz-Sabater et al., 2021).

The main objective of this work is to study the trend of SM in Europe during the last three decades (1991 to 2020). The studies published thus far on the SM trend have been on a global scale, focusing the analysis on areas of special interest such as the Sahel, Australia, India or North America (Sheffield and Wood, 2007). However, too little attention has been given to Europe despite the expected increased risk of drought on the continent (Naumann et al., 2021). The second objective of the study is the comparison between a rank-based and an empirical decomposition approach in the analysis of SM trends. For these purposes, SM trends from two databases, one from modelling and the other from reanalysis, have been studied over Europe. Two methods were used: a widely used method based on monotonic behavior, the Mann-Kendall (MK), and a novel nonlinear method, the empirical mode decomposition (EMD). The statistical significance of trends and their signs were evaluated in the different types of climate, according to the Köppen-Geiger classification. In addition, the study was conducted at different time scales (monthly and annually) to gain a full understanding of the changes in temporal SM temporal dynamics that occurred in Europe during the last 30 years, from 1991 to 2020.

2. Dataset and methods

2.1. Soil moisture data

Two different SM databases were used, both provided by the Copernicus Climate Change Service (C3S) but with different sources and characteristics. On the one hand, the European Centre for Medium-Range Weather Forecasts (ECMWF) reanalysis project ERA5-Land provides several land variable series, including SM. The land surface reanalysis describes the water and energy cycles over land by using the Hydrology Tiled ECMWF Scheme for Surface Exchanges over Land (HTESSEL) (Balsamo et al., 2009), and derives the atmospheric forcing from ERA5 (Muñoz-Sabater et al., 2021). ERA5-Land (for simplicity, hereafter ERA5L) is indirectly influenced by several sources of assimilated observations, satellite and in situ (Hersbach et al., 2020), through the atmospheric forcing. The series are provided from 1981 to the present with hourly temporal resolution and a regular grid of 0.1°. SM is estimated in 4 depth layers from 0 to 289 cm. In this work, only surface (0–7 cm) SM was studied; thus, only the first layer of the product and the data at 12 am and 12 pm were used.

On the other hand, the SM series from the hydrological rainfall-runoff model Lisflood (LF) were also used. This model was developed by the floods group of the Natural Hazards Project of the Joint Research Centre (JRC) of the European Commission (Van Der Knijff et al., 2010) and is used in the Copernicus European Drought Observatory (EDO) (https://edo.jrc.ec.europa.eu) and the European Flood Awareness System (EFAS) (Smith et al., 2016). The model can simulate the long-term water balance by considering several processes such as snow melt, infiltration, interception of rainfall, evaporation or soil moisture exchange between the soil layers, among others (van Der Knijff et al., 2010). In this work, the dataset produced by EFAS was used, which was produced with gridded observational meteorological data (Smith et al., 2016). The SM series are provided daily since 1991 to present with a spatial resolution of 5 × 5 km (de Roo et al., 2000). SM is estimated for 3 depth layers, but only the first layer, which refers to the first 5 cm of the soil, was considered in this study.

Both databases have been validated (Laguardia and Niemeyer, 2008; Li et al., 2020) and widely used for several applications (González-Zamora et al., 2021; Zhang et al., 2021), including the study of SM trends (Almendra-Martín et al., 2021a; Cammalleri et al., 2016). Validation studies have shown accurate estimations of SM for both products in the region of study except for high latitudes and the Alps because of the poor performance in heterogeneous landscapes and topography regions, the presence of ice cover and the limited availability of satellite data (Laguardia and Niemeyer, 2008; Li et al., 2020). In this work, a comparison between both products was conducted (results not shown). The LF database was resampled into the ERA5L grid by calculating the spatial average, and the series were compared. A good correlation was obtained, with a median value of Pearson correlation coefficient of 0.67. The poorest values were obtained for the Alps and the Scandinavian Peninsula, in line with previous works (Laguardia and Niemeyer, 2008; Li et al., 2020). Therefore, these regions were filtered using auxiliary databases.

Taking all of this into account, trends of SM anomaly series were evaluated for the study period, 1991–2020, and the monthly and annual temporal scales were analyzed. Thus, first, the daily series of both products were averaged into these scales. Then, anomalies were calculated by subtracting the monthly and annual mean calculated using the entire period of study for each pixel.

2.2. Auxiliary data and mask

Some regions were excluded from the study due to different factors, such as irrigation management, areas with permanent or seasonal ice cover or regions where estimations of SM are not such accurate. For this reason, ancillary databases were used to create a mask that filters these areas.

For the irrigated areas, the Digital Global Map of Irrigation Areas of the Food and Agriculture Organization (FAO) was used. It consists of a global map with a spatial resolution of 5 arc minutes that provides the percentage area irrigated (Siebert et al., 2005). In this study, pixels with >10% irrigation area were masked.

The Köppen-Geiger classification was used both to study the distribution of SM anomaly trends in the different European climates and to mask regions with less accurate SM values due to the presence of ice cover. This classification uses 3 categories to describe the various types of climates worldwide (Peel et al., 2007). The first category contains 5 main classes that are subdivided into 30 different types of climates. In this work, the map developed by Beck et al. (2018) with a spatial resolution of 1 km was used. This map was resampled into LF and ERA5L grids using a majority filter. The rest of the climate subdivisions were merged into their more general categories until each class represented at least 1% of the area of study.

Therefore, the mask was created by incorporating all the pixels considered irrigated areas and those with polar and cold – without dry season – very cold winter climate. In this way, those regions with low accuracy SM estimations for both products are excluded. The final classification used to study the SM trend distribution is shown in Table 1, and a map with the spatial distribution of each class is shown in Fig. 1.

2.3. Drought attributes series

Since SM changes have a direct impact on the various types of droughts, their trends were also studied by analyzing the main attributes that characterize drought, namely, onset, duration and intensity. According to Sheffield and Wood (2007), a drought is defined as a period with SM quantile values below an arbitrary threshold. In this study, the threshold was set in the 10th percentile (q_{10}) of the daily series of each pixel, corresponding to severe drought (Sheffield and Wood, 2008). Annual series were obtained for each attribute. Thus, duration (D) was calculated as the number of days in a year that SM had values below q_{10}. Onset series were calculated as the first day of the year on which SM presented a value below the threshold and was maintained for at least seven consecutive days. The 7-day criterium was chosen to avoid a flash drought ocurring before the dry season from setting the representative onset of a specific year. Finally, intensity series were calculated as the mean magnitude over the drought duration of each year, with the magnitude of the deviation below the threshold.

2.4. Trend analysis

Hydrological trend identification is a challenging task usually investigated under the assumption of monotonic behavior in their interannual changes (Sang et al., 2013), but hydroclimatic series are known to change nonmonotonically. Linear trends can be heavily influenced by the period and the temporal scale of the study (Pan et al., 2019; Sang et al., 2018). Monotonic approximations, in turn, have also been proposed to study hydroclimatic series trends in the literature and have shown consistent results (Albergel et al., 2013; Dorigo et al., 2012; Li et al., 2015). In this work, two methodologies were considered to evaluate SM anomaly trends to consider both strategies, monotonic and nonmonotonic. Both methods were applied to the entire annual and monthly series of SM anomaly. In addition, interannual changes were computed for SM anomaly series by separately analyzing trends for each month.

Table 1
Percentages of coverage in Europe of each Köppen-Geiger climate type and the mask used in the study in both SM databases spatial resolution.

Köppen-Geiger	LF (%)	ERA5L (%)
Cold - without dry season - warm summer (Dfb)	44	46
Cold - without dry season - hot summer (Dfa)	3	3
Temperate - without dry season (Cf)	22	22
Temperate - dry summer (Cs)	9	8
Arid (B)	5	5
Mask	18	17

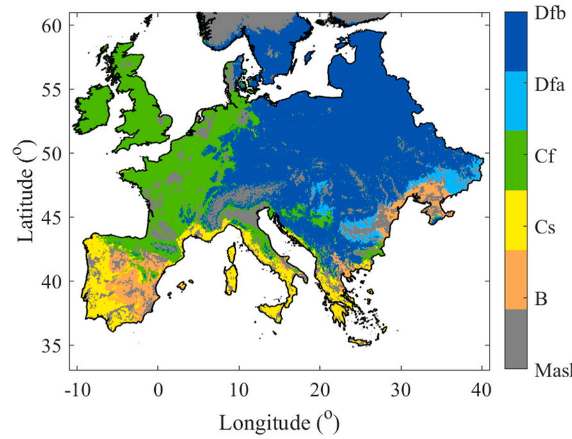

Fig. 1. Spatial distribution of the Köppen-Geiger climate types and the mask used in the study.

2.4.1. Mann-Kendall test

The MK test (Kendall, 1948; Mann, 1945) is a nonparametric test widely used to detect trends. It identifies the monotonic upwards or downwards trend of a series and determines if it has statistical significance at a given level. The null hypothesis assumes that a given series has no trend, i.e., it is independently distributed. To accept or reject the null hypothesis, the statistic S, which determines the sign of the trend, is calculated of the following form:

$$S = \sum_{i=1}^{n-1} \sum_{j=i+1}^{n} sgn\left(x_j - x_i\right) \tag{1}$$

where x refers to the points of a series of lengths n, and $sgn()$ is the sign function that makes the test robust against outliers (Asfaw et al., 2018). The significance of the trend at a given significance level is given by the Z parameter obtained as follows:

$$Z = \begin{cases} \dfrac{S-1}{\sqrt{var(S)}} & S > 0 \\ 0 & S = 0 \\ \dfrac{S+1}{\sqrt{var(S)}} & S < 0 \end{cases} \tag{2}$$

where var refers to the variance. In this study, the significance level was set to 0.05, which implies that with absolute values of Z >1.96, the null hypothesis is rejected, and the trend can be considered significant. One limitation of the MK is the chance of obtaining a significant trend with autocorrelated series (Hamed and Rao, 1998); however, we deal with this problem here by analyzing the anomalies of SM series, which is a common practice to avoid seasonal effects when analyzing SM trends (Albergel et al., 2013).

2.4.2. Empirical Mode Decomposition

The EMD is a method developed by Huang et al. (1998) for the analysis of nonlinear and nonstationary data. It allows the decomposition of a series into a number of intrinsic mode functions (IMFs) by empirically identifying the intrinsic oscillatory modes (Fig. 2a). An IMF meets that (i) its number of extrema and its number of zero crossings must either be equal or differ at most by one, and that (ii) at any point, the mean value of the envelopes defined by the local maxima and by the local minima is zero (Narayanankutty et al., 2010). The decomposition is performed through a shifting process using only local extrema. For a

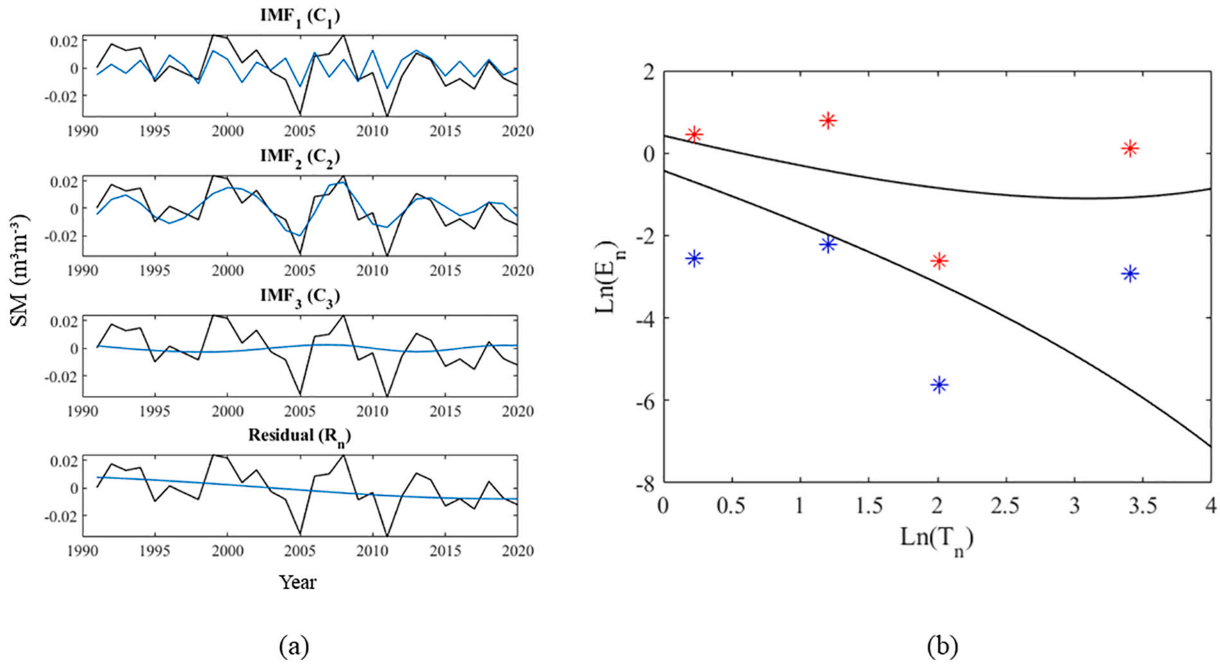

Fig. 2. EMD is applied to an annual SM anomaly series as an example. (a) IMFs C1, C2 and C3 and the residual Rn (blue) obtained in the decomposition of a series *x* (black). (b) Representation of the a priori (blue stars) and a posteriori (red stars) significance tests with the spread lines at a 95% confidence level (black lines). (For interpretation of the references to colour in this figure legend, the reader is referred to the web version of this article.)

signal $x(t)$, first, all the local extrema are identified. These local maxima and minima are connected with a suitable curve-fitting method. In this work, the piecewise-cubic Hermite interpolation polynomials method was used. The first component is obtained by subtracting the local mean curve of the upper and lower envelopes. The obtained component is treated as the original signal, and these steps are repeated until the envelopes are symmetric with respect to zero mean under certain criteria (Wu and Huang, 2009). The final component is designated as one IMF (C_i), and it is defined as follows: $r_0 = x(t) - C_i$. The shifting process is repeated using r_0 as the signal, and it is completed when the last component obtained becomes a monotonic function, the residual (R_n), from which no more IMF can be extracted. Thus, the EMD decomposes a signal $x(t)$ of the following form:

$$x(t) = \sum_{i}^{n} C_i + R_n \tag{3}$$

where the residual R_n represents the monotonic trend of the entire period of the series. This resulting trend is analyzed, as in the MK method, by its sign and its significance.

To differentiate the IMFs that provide a physically meaningful representation of the fundamental processes from those that represent the inherent noise in the data, characteristics of noise need first to be established (Wu and Huang, 2005). Wu and Huang (2004, 2005) studied the characteristics of white noise by using EMD and proposed a method to test the statistical significance based on deduced analytic expressions that describe the statistical characteristics of white noise. Thus, as the IMFs separate physical processes of a series at various time scales and give its temporal variation without a linear assumption, the mean period of the nth IMF (T_n) can be estimated as the ratio between the number of data (N) and the number of extrema of the series:

$$T_n = \frac{N}{N^{\circ}\ extrema} \tag{4}$$

And the energy density (E_n) of the nth IMF (C_n) is defined as:

$$E_n = \frac{1}{N}\sum\nolimits_{j=1}^{N} [C_n(j)]^2 \tag{5}$$

The authors established the spread of the energy densities of white noise by using the Monte Carlo method for different series of length (N). With this, they studied the relationship between the mean period (T_n) and the energy density (E_n) and defined its spread function. In this way, they designed a test to evaluate the significance of each IMF. First, the normalized series (between −1 and 1) is decomposed using EMD (Fig. 2a), and the mean period and the energy density of each component is obtained. Then, the upper and lower lines of the spread function (black lines in Fig. 2b) of the energy distribution at a confidence level are calculated using the analytical expressions defined in Wu and Huang (2004). Finally, the energy density of the IMFs and the spread function are compared (blue stars in Fig. 2b), if the energy is located between the upper and lower limits should be considered to contain just noise. However, this is an a priori test, in which the noise level of the data is unknown. For series in which it can be established that an IMF is just noise as it contains little useful information (IMF$_1$), its energy can be assigned to the 99% confidence upper line (Wu and Huang, 2005). With its energy, the energies of the other IMFs are rescaled (red stars in Fig. 2b). In this a posteriori tests, the upper line of the spread function (upper black line in Fig. 2b) sets the significance threshold. The IMFs with an energy above the threshold have physically meaningful representation. The a posteriori test has been verified and is widely used to lay the significance down when using the EMD (Adarsh and Janga Reddy, 2019; Lee and Ouarda, 2011; Wu and Huang, 2005). To evaluate the significance of the trend, this test was applied to the residual as in Sang et al. (2014).

3. Results and discussion

3.1. Annual and monthly soil moisture anomalies trends

The results for both trend analysis (MK and EMD) and SM products (ERA5L and LF) consistently agree on a general prevalence of negative trends, regardless of the type of climate, which implies a change to drier conditions in most parts of the European continent during the last 30 years (Figs. 3 and 4). In general, the EMD method detects more significant trends than MK, and the increase in significant trends when using

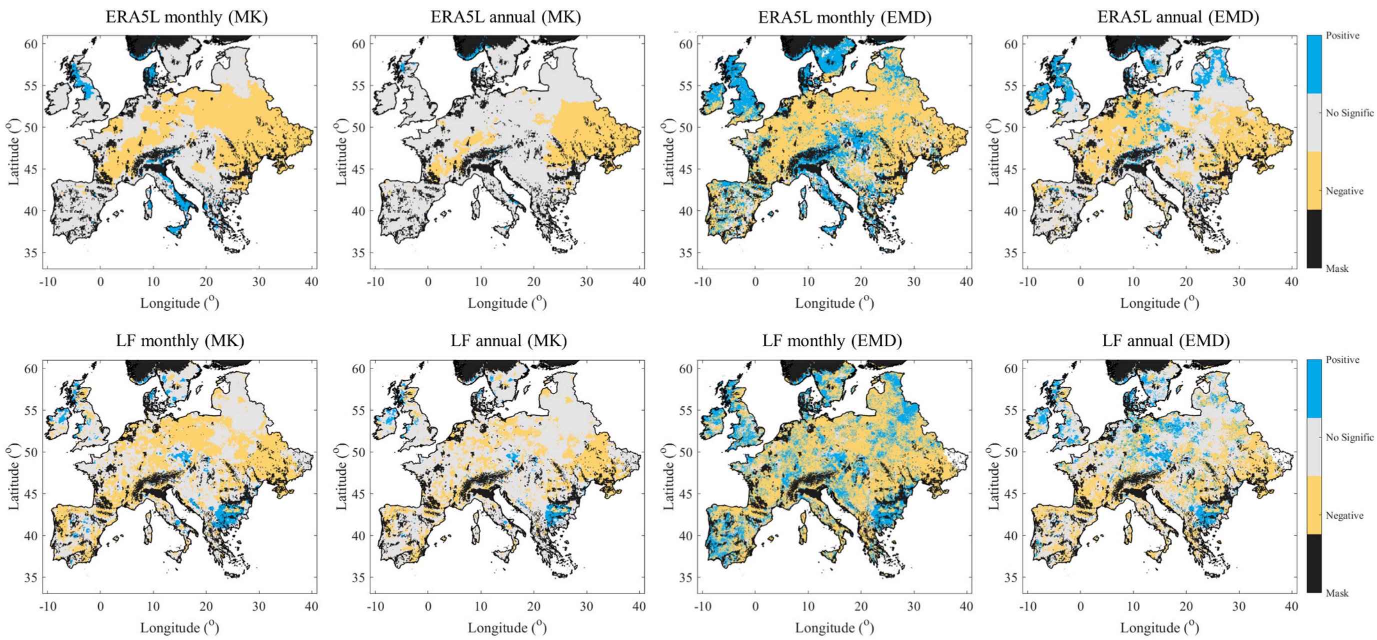

Fig. 3. Spatial distribution of soil moisture anomaly trends obtained with ERA5L and LF for monthly and annual series using MK and EMD methods.

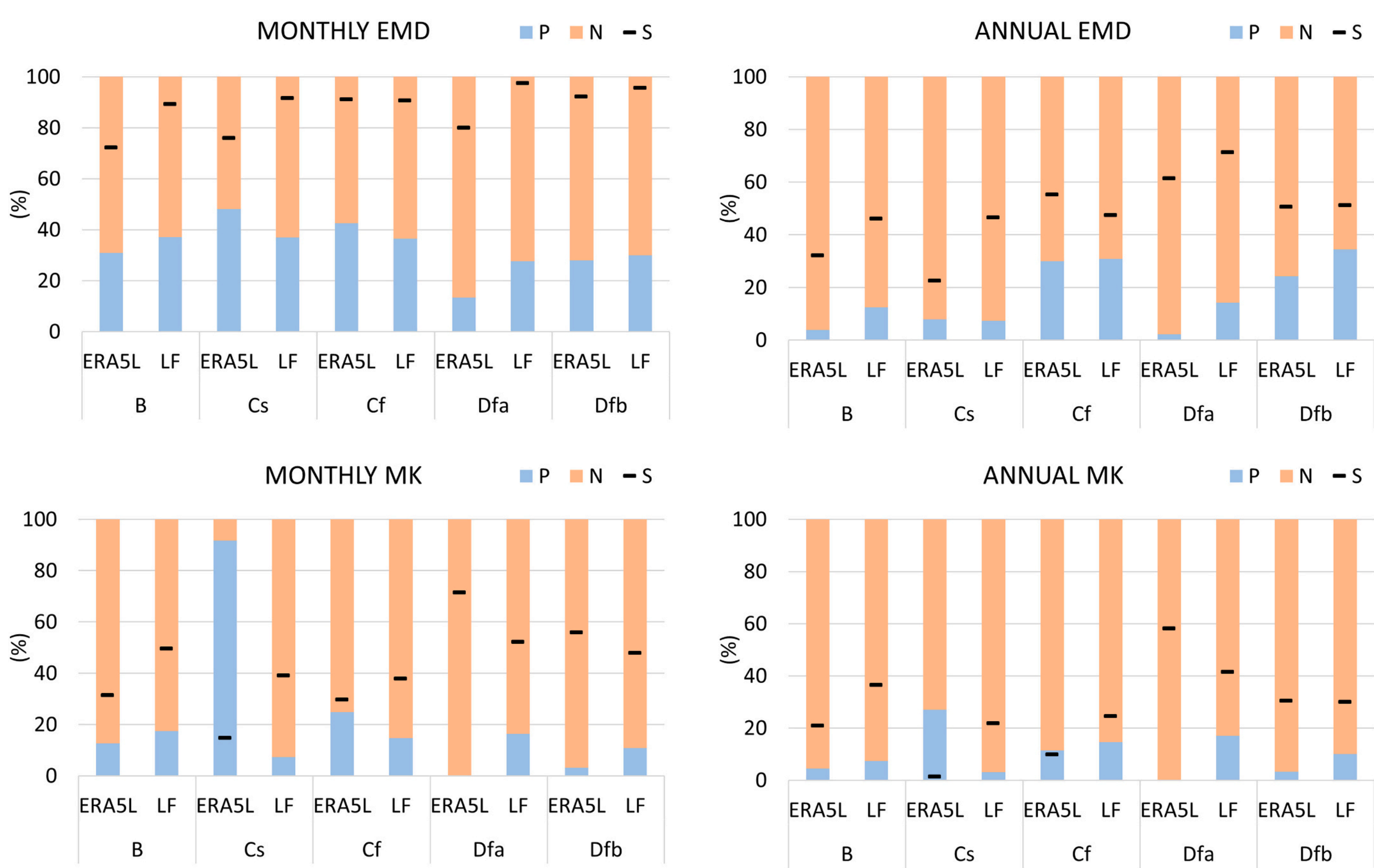

Fig. 4. Percentage of pixels with significant trends (S, black line) and percentage of positive (P, blue bar) or negative (N, orange bar) trends regarding the significant ones, of each SM database and Köppen-Geiger climate regions in Table 1. The results are shown for the two methods, EMD and MK, and the two temporal scales, monthly and annual. (For interpretation of the references to colour in this figure legend, the reader is referred to the web version of this article.)

EMD is associated with an increase in positive trends. This fact could be related to the magnitude of these trends, since the MK does not have the power to detect small trends masked by other components of the series (Sang et al., 2014). This may imply that in regions showing an increase of SM with the EMD but not with MK, the components of the series with a nonmonotonic behavior have more weight than its long-term trend.

The spatial distribution of the obtained trends (Fig. 3) indicates great consistency between the methods and temporal scales of the analysis.

With both SM products, positive trends are mainly obtained in Scotland and northern Ireland, which implies a change to wetter conditions, similar to what Bordi et al. (2009) obtained. Changes to drier conditions are located in central and eastern Europe, in line with previous studies (Jaagus et al., 2021; Trnka et al., 2009). Thus, regions that show a wetting trend are generally located at higher latitudes, in areas where the average moisture content is higher, and drying trends are generally located in central and southern Europe. This is in line with the "dry gets drier, wet gets wetter" trend paradigm studied by Feng and Zhang (2015). In contrast, very few and limited regions show distinct trends depending on the SM product used, such as Bulgaria, where a positive trend dominates with LF, and a negative trend with ERA5L or the Italian Peninsula, where a negative trend is observed in monthly series with LF but positive with ERA5L.

At temporal scales, the MK method shows more trends that are significant in monthly series than in annual series. This could be related to the fact that the MK depends on the sample size as well as on the magnitude of the trend to be identified (Adamowski et al., 2009; Sang et al., 2014). However, this difference is also observed when using EMD. This implies fewer interannual changes in this variable, similar to what Piles et al. (2019) and Vicente-Serrano et al. (2021) saw when they analyzed SM and droughts trends respectively. In the literature, trends have usually been analyzed at annual or seasonal scales and assuming monotonic behavior; thus, significant long-term trends have barely been observed in Europe (Albergel et al., 2013; Dorigo et al., 2012; Feng and Zhang, 2015).

The distribution of trends according to the type of climate is quite similar. Although some patterns are observed, in all cases, they imply a change to drier conditions (Fig. 4). In general, higher percentages of significant trends are located in regions with cold climates (Dfa and Dfb). When using MK, regions with temperate climates (Cs and Cf) present the lowest percentages of significant trends, while with the EMD, this pattern is not observed. Attending to products, higher percentages of significant trends in arid climate areas (B) and temperate with dry summer climate areas (Cs) are observed with LF. Finally, when comparing temporal scales, at monthly scale Cs region shows an abnormal positive trend percentage with ERA5L associated with positive trends obtained in Italy; however, although the number of significant trends is very low, a high percentage of positive trends are also obtained with this product at monthly scale with EMD.

Comparative tables were elaborated to quantify the differences between the results obtained with two methodologies (Table 2), temporal resolutions (Table 3), and products, similar to Qiu et al. (2016), but analyzing only pixels with a significant trend. The match rate is always higher than the discrepancies, with the negative trends being more consistent. On the one hand, when comparing both methods, it is observed that EMD tends to detect positive trends that MK considers negative (Table 2). Sang et al. (2014) obtained similar results when analyzing precipitation series, and they observed that the MK test underestimated the upwards trend. On the other hand, trends obtained with various temporal scales applying MK present no discrepancies; however, the number of coinciding significant trends is very low. In contrast, with EMD, higher values of significant trends are obtained, and therefore, discrepancies increase, with its total percentage being greater than that of positive coincident trends. These discrepancies again suggest that changes to wetter conditions are occurring slightly enough to be masked by nonmonotonic components of the series.

Table 2
Comparison of the percentage of trends obtained with the two methods, MK and EMD, for the two SM databases used at annual and monthly time scales. Sign "+" indicates positive and significant trends, and sign "-" indicates negative and significant trends.

		ERA5L		LF	
		MK +	MK -	MK +	MK -
Monthly	EMD +	9	7	11	11
	EMD -	1	83	1	77
Annual	EMD +	3	2	12	7
	EMD -	0	95	0	81

Table 3
Comparison in percentage of trends obtained for the two timescales, annual (A) and monthly (M), for the two methods and SM databases used. Sign "+" indicates positive and significant trends, and sign "-" indicates negative and significant trends.

		ERA5L		LF	
		M +	M -	M +	M -
EMD	A +	15	9	16	12
	A -	12	64	11	61
MK	A +	3	0	10	0
	A -	0	97	0	90

3.2. Monthly pattern of soil moisture anomalies trends

Despite the general consistency between results when using different approaches, some variations have been observed that deserve particular attention. The most notable ones were obtained when studying trends of the series with different temporal resolutions using the empirical decomposition method. To clarify these differences, a dedicated analysis of monthly changes and trends was performed. This approach revealed that most changes in SM are not uniform among the year. For simplicity, only results obtained with the EMD are shown (Figs. 5 and 6), since very few significant trends were obtained with MK for this analysis.

Again, trends obtained with both SM products are consistent. An increase in significant negative trends is obtained in April over almost the entire continent with both products, which implies a general decrease in SM during this month. These results are in concordance with several studies that have detected drier springs in Europe over the last decades (Jaagus et al., 2021; Trnka et al., 2009; Vautard et al., 2007). In contrast, an increasing trend of SM is obtained in the Iberian Peninsula for that same month, similar to what Almendra-Martín et al. (2021a) observed using a rank-based approach. The same wet pattern in the Iberian Peninsula (IP) and dry pattern elsewhere in Europe were obtained when analyzing precipitation trends of climatic research unit (CRU) monthly anomaly series (Fig. S1), which reinforces our obtained results with SM time series, i.e., a change in trend to wetter conditions in April and May in the IP.

In addition, the percentage of significant trends rises during autumn (September–October-November) for both products and in the winter (December–January-February) for the LF product (Fig. 6). Between these months, there is a fluctuation in the sign of the trends obtained, which emphasizes the nonmonotonic behavior of SM at this temporal scale. November and January show a predominance of decreasing trends in most of the European territory, while for December and February, increasing trends in SM anomalies are mainly observed. However, a constant pattern of increase in SM trends is obtained for the winters in the northeastern region (Estonia, Latvia, Lithuania and Belarus), in concordance with what Cammalleri et al. (2016) obtained and with the increase in the winter precipitation observed by Jaagus et al. (2021) in this region. A decrease in significant trends is observed in the summer (June–July-August) months; however, there is a predominance of negative trends.

3.3. Drought attribute trends

Trends in SM anomaly series have been detected; thus, changes in related drought characteristics could be expected. To verify this, a similar analysis using MK and EMD was conducted on drought attributes annual series of ERA5L and LF to identify their changes during the last three decades. The EMD method also detected more significant trends

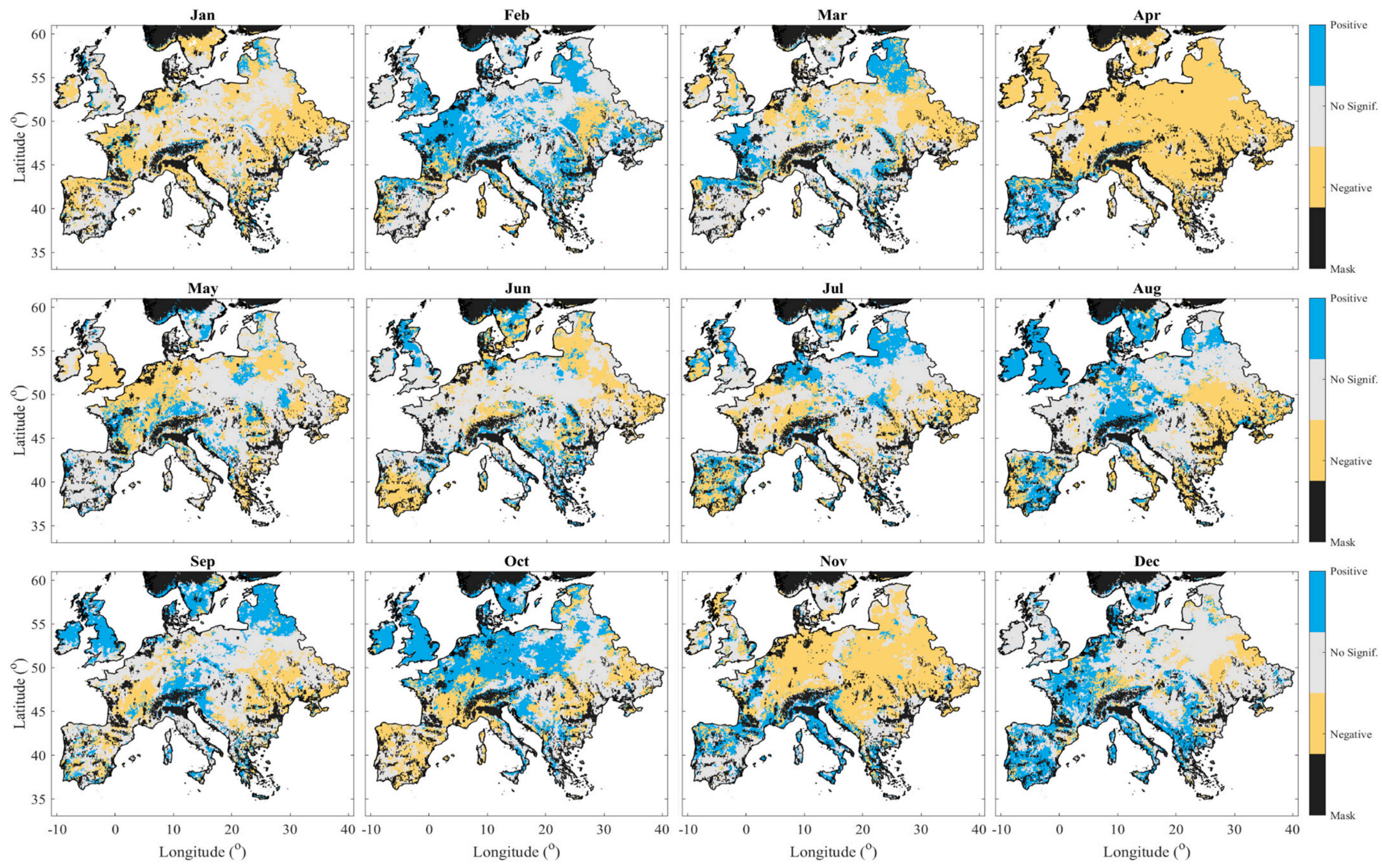

Fig. 5. Spatial distribution of SM anomaly trends (EMD) obtained with monthly ERA5L series for each month.

than MK, but more importantly, our results obtained with both methods show a general increase in the duration and intensity of extreme droughts over the European continent (Fig. 7). These results are in agreement with the expected evolution based on climate change models under different scenarios (Giorgi and Lionello, 2008; Grillakis, 2019; Spinoni et al., 2018). In addition, our results indicate that the onset of extreme drought events, in general, tends to be delayed a few days per year in some regions, especially with ERA5L in arid and temperate regions (Fig. S2).

In this analysis, the increase in significant trends when using EMD is associated with a slightly increase in negative trends for intensity and duration attributes, which implies a change to shorter and less intense droughts in some regions, mainly in Cf and Dfb climates. Again, we could only detect these changes with the empirical decomposition method and not with the MK approach, which suggests the convenience of using methods that account with nonmonotonic behavior to analyze the trend in soil moisture anomalies.

When each type of climate trend is analyzed, different patterns in drought trends are observed. Cf, Dfa and Dfb refer to climates without a dry season; therefore, lower changes in droughts should be expected. Indeed, the results obtained with the intensity series present the lowest percentages of significant trends, and almost half of them show a decreasing trend in intensity with EMD in Cf and Dfb. However, there is a general increase in the duration of droughts in these regions, and the start of drought events tends to advance in temperate climate Cf and some regions with a Dfb climate. A clear pattern is observed in arid regions and regions with more intense, longer and increasingly delayed extreme droughts, although the number of significant results depends upon the SM product used, as LF detects more trends in duration series but less in onset than ERA5L. Similar results were obtained in regions with a Cs climate.

This general increase in the duration and intensity of extreme droughts is consistent with several changes observed in the precipitation behavior over Europe in prior studies (de Luis et al., 2011; Hänsel et al., 2019; Hynčica and Huth, 2019), alongside the rise of average temperature (Trenberth, 2011) and the consequent increase in potential evapotranspiration, which, in turn, causes an increase in extreme events such as droughts (Hänsel et al., 2019; Jaagus et al., 2021).

4. Conclusions

In this work, the trend of SM in Europe in the last three decades was investigated using rank-based and empirical decomposition approaches. For this, two SM databases, one from modelling (LF) and the other from reanalysis (ERA5L), were used. Anomaly series of SM were calculated at monthly and annual temporal scales and were analyzed using two approaches: monotonic (MK) and nonmonotonic (EMD). Strong consistency was observed between the results of both databases, methods and temporal scales. The distribution of SM anomaly trends in the different European climates was also studied, and no clear pattern was identified. The results showed a general change trend to drier conditions, mainly located in Central and Eastern Europe. Although the MK method has been widely used to study the trends of SM, the empirical decomposition approach detected more significant trends. The patterns in SM that could be identified only with EMD are in accordance with changes observed in other hydroclimatic variables on this continent during recent decades, such as temperature, precipitation or evaporation. Furthermore, many of the trends observed with EMD and not with MK are positive, while negative trends are more consistent with both methods. This suggests that changes to wetter conditions can be masked by a nonmonotonic behavior of the series.

The most notable differences in SM trends were obtained when comparing the results at monthly and annual scales, especially when using the EMD method. Less significant trends were observed at annual

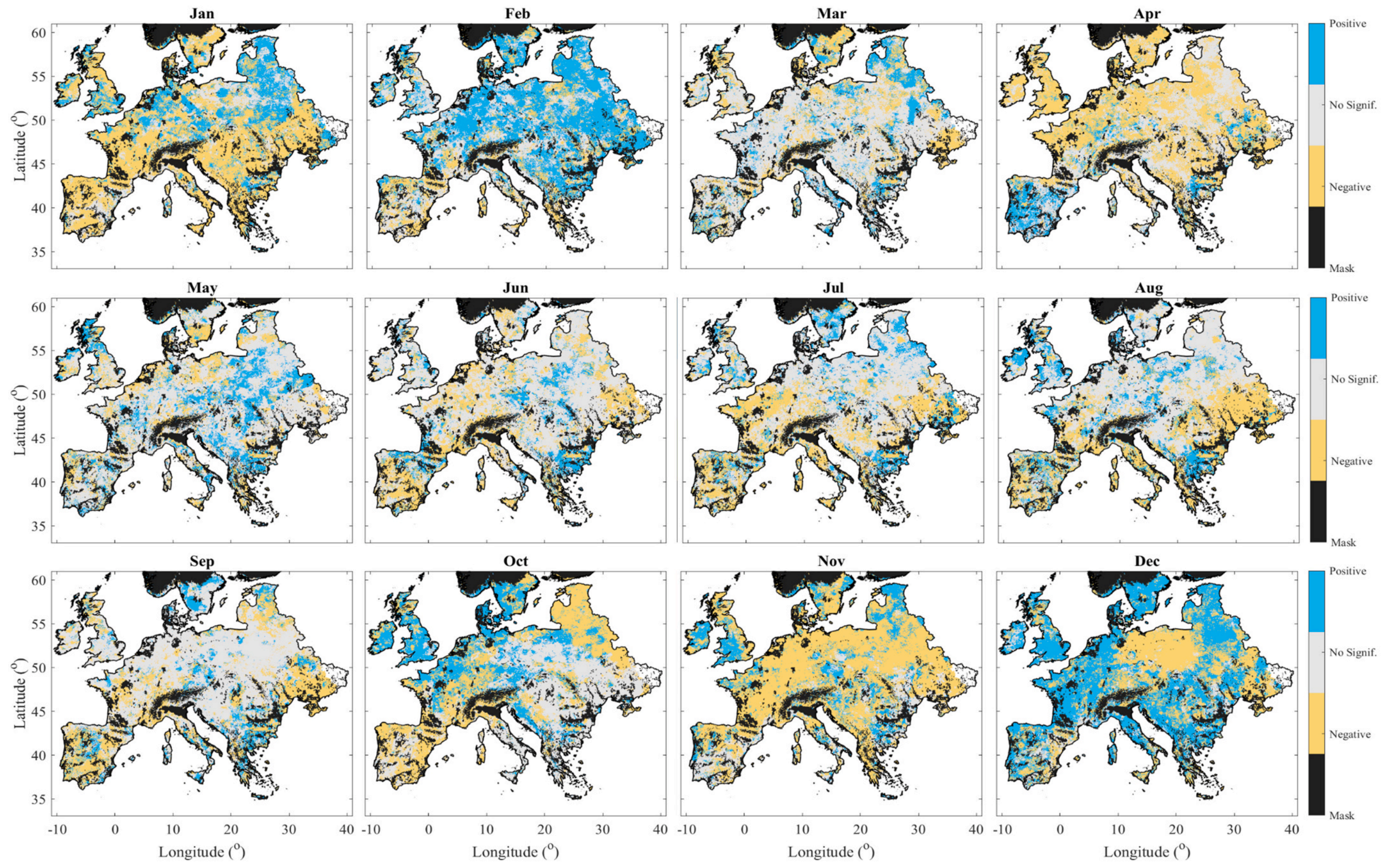

Fig. 6. Spatial distribution of SM anomaly trends (EMD) obtained with monthly LF series for each month.

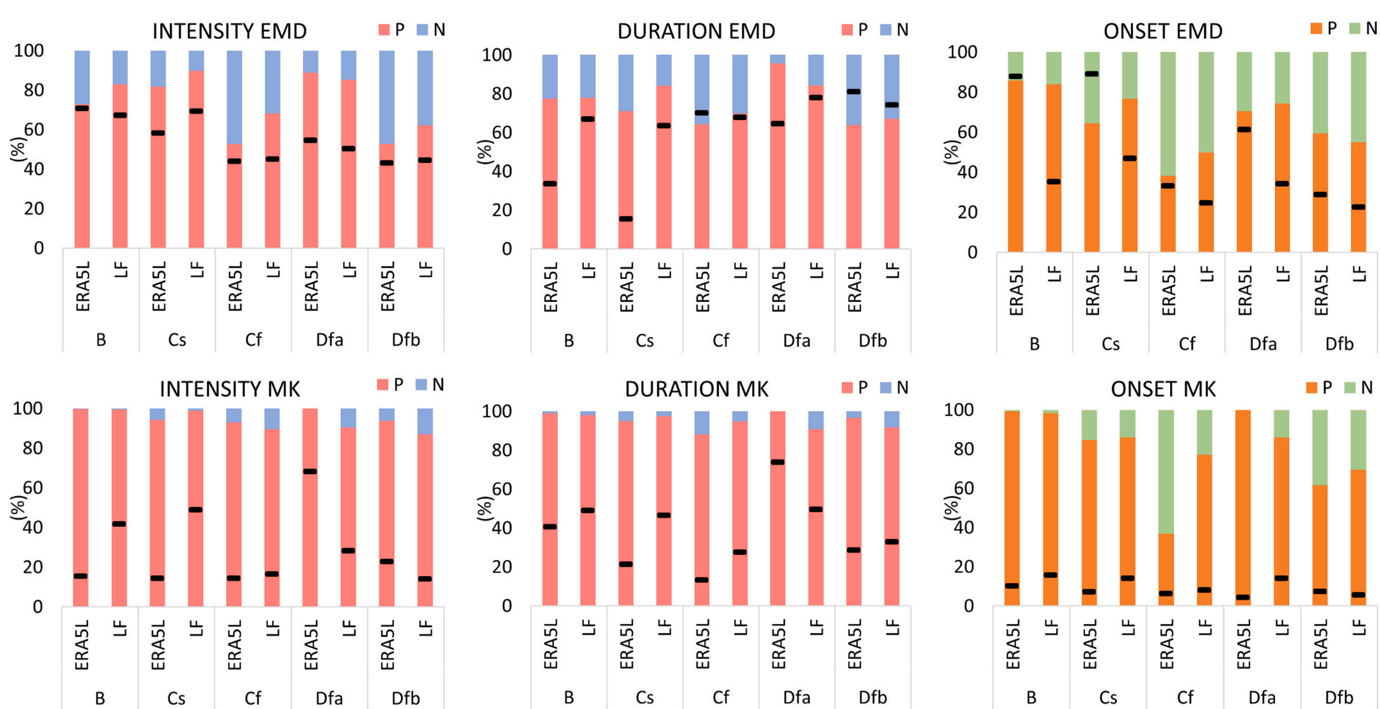

Fig. 7. Percentage of pixels with significant trends (S, black line) and percentage of positive (P, blue bar) or negative (N, orange bar) trends regarding the significant ones, of duration, intensity and onset annual series of each SM database in each Köppen-Geiger type of climate. The results obtained with the two methods, EMD and MK. (For interpretation of the references to colour in this figure legend, the reader is referred to the web version of this article.)

than at monthly scales, but significant ones showed in some regions different signs depending on the temporal scale. To further scrutinize this mismatch, interannual changes for each month series were analyzed using the EMD method. A general decreasing trend in SM anomalies was obtained in April over the entire continent, which implies a trend towards drier springs in Europe. Just the Iberian Peninsula showed the opposite behavior with an increasing trend of SM in April. Autumn and winter months showed a fluctuation in the sign of the trends, which emphasizes the nonmonotonic behavior of changes in this variable in the months when the average SM is the highest. In contrast, summer months showed fewer significant trends; however, the significant trends indicate a trend towards drier conditions.

As several changes were observed in the SM series, related changes in the characteristics of drought events could also be expected. To evaluate this hypothesis, the duration, intensity and onset annual trends of extreme droughts in Europe were studied. The results showed a prevalence of an increase in the duration and intensity of extreme droughts and a few days of delayed onset per year. However, some change patterns in the different climate regions of Europe could be observed only with the EMD method. Areas with climates without dry season (Cf, Dfa and Dfb) showed the lowest percentage of significant trends in intensity series, and almost half of the area showed a decreasing trend. However, the duration of extreme droughts showed a general increasing trend, especially in the coldest regions (Dfb). In arid regions, a clear pattern of increasingly longer, more intense and delayed extreme droughts was observed. In this analysis, the EMD method again detects more trends than MK, in particular, the negative (drier conditions) trends.

SM trends have been commonly studied through approaches that just account for the monotonic change and at large temporal scales. This has resulted in few to no changes in patterns being detected when analyzing this variable in Europe during recent decades. However, trends in related variables such as temperature or precipitation have been observed due to the impact of climate change, so changes could also be expected in SM. The empirical decomposition approach used in this work has revealed a large number of trends that show a general decreasing SM pattern in Europe, reconciling the results previously reported in the literature when analyzing the trends in intimately linked variables such as temperature, precipitation or evaporation. The results of this work prove that empirical decomposition approaches allow to account for the nonmonotonic behavior of the series and can be a suitable tool to understand the changes in SM dynamics, as well as the impact of climate change on this variable, which could be instrumental to better understand subsequent changes in the Earth's water cycle.

Declaration of Competing Interest

The authors declare that they have no known competing financial interests or personal relationships that could have appeared to influence the work reported in this paper.

Acknowledgements

This study was supported by the Spanish Ministry of Science and Innovation (projects ESP2017-89463-C3-3-R and PID2020-114623RB-C33), the Castilla y León Government (projects SA112P20 and CLU-2018-04) and the European Regional Development Fund (ERDF). The research of Laura Almendra-Martín was funded by a pre-doctoral grant (Castilla y León Government and ERDF).

Appendix A. Supplementary data

Supplementary data to this article can be found online at https://doi.org/10.1016/j.gloplacha.2022.103868.

References

Adamowski, K., Prokoph, A., Adamowski, J., 2009. Development of a new method of wavelet aided trend detection and estimation. Hydrol. Process. 23, 2686–2696.
Adarsh, S., Janga Reddy, M., 2019. Evaluation of trends and predictability of short-term droughts in three meteorological subdivisions of India using multivariate EMD-based hybrid modelling. Hydrol. Process. 33 (1), 130–143.
Albergel, C., Dorigo, W., Reichle, R.H., Balsamo, G., De Rosnay, P., Muñoz-Sabater, J., Isakse, L., De Jeu, R., Wagner, W., 2013. Skill and global trend analysis of soil moisture from reanalyses and microwave remote sensing. J. Hydrometeorol. 14 (4), 1259–1277.
Almendra-Martín, L., Martínez-Fernández, J., González-Zamora, Á., Benito-Verdugo, P., Herrero-Jiménez, C.M., 2021a. Agricultural drought trends on the Iberian Peninsula: an analysis using modeled and reanalysis soil moisture products. Atmosphere 12 (2), 236.
Almendra-Martín, L., Martínez-Fernández, J., Piles, M., González-Zamora, Á., 2021b. Comparison of gap-filling techniques applied to the CCI soil moisture database in Southern Europe. *Remote Sens.* Environ. 258, 112377.
An, R., Zhang, L., Wang, Z., Quaye-Ballard, J.A., You, J., Shen, X., Gao, W., Huang, L., Zhao, Y., Ke, Z., 2016. Validation of the ESA CCI soil moisture product in China. Int. J. Appl. Earth Obs. Geoinf. 48, 28–36.
Asfaw, A., Simane, B., Hassen, A., Bantider, A., 2018. Variability and time series trend analysis of rainfall and temperature in northcentral Ethiopia: a case study in Woleka sub-basin. Weather. Clim. Extreme 19, 29–41.
Bai, L., Xu, J., Chen, Z., Li, W., Liu, Z., Zhao, B., Wang, Z., 2015. The regional features of temperature variation trends over Xinjiang in China by the ensemble empirical mode decomposition method. Int. J. Climatol. 35 (11), 3229–3237.
Balsamo, G., Beljaars, A., Scipal, K., Viterbo, P., van den Hurk, B., Hirschi, M., Betts, A.K., 2009. A revised hydrology for the ECMWF model: verification from field site to terrestrial water storage and impact in the integrated forecast system. J. Hydrometeorol. 10 (3), 623–643.
Beck, H.E., Zimmermann, N.E., McVicar, T.R., Vergopolan, N., Berg, A., Wood, E.F., 2018. Present and future Köppen-Geiger climate classification maps at 1-km resolution. Sci. Data 5 (1), 1–12.
Bordi, I., Fraedrich, K., Sutera, A., 2009. Observed drought and wetness trends in Europe: an update. Hydrol. Earth Syst. Sci. 13 (8), 1519–1530.
Bueso, D., Piles, M., Camps-Valls, G., 2020. Nonlinear PCA for spatio-temporal analysis of Earth observation data. IEEE Trans. Geosci. Remote Sens. 58 (8), 5752–5763.
Cammalleri, C., Micale, F., Vogt, J., 2016. Recent temporal trend in modelled soil water deficit over Europe driven by meteorological observations. Int. J. Climatol. 36 (15), 4903–4912.
Carmona, A.M., Poveda, G., 2014. Detection of long-term trends in monthly hydro-climatic series of Colombia through Empirical Mode Decomposition. Clim. Chang. 123 (2), 301–313.
Cheng, S., Huang, J., 2016. Enhanced soil moisture drying in transitional regions under a warming climate. J. Geophys. Res. Atmos. 121 (6), 2542–2555.
Cheng, S., Huang, J., Ji, F., Lin, L., 2017. Uncertainties of soil moisture in historical simulations and future projections. J. Geophys. Res. Atmos. 122 (4), 2239–2253.
Dai, A., 2013. Increasing drought under global warming in observations and models. Nat. Clim. Chang. 3 (1), 52–58.
de Luis, M.D., Gonzalez-Hidalgo, J.C., Brunetti, M., Longares, L.A., 2011. Precipitation concentration changes in Spain 1946–2005. Nat. Hazards Earth Syst. Sci. 11 (5), 1259–1265.
de Roo, A.P.J., Wesseling, C.G., Van Deursen, W.P.A., 2000. Physically based river basin modelling within a GIS: the LISFLOOD model. Hydrol. Process. 14 (11−12), 1981–1992.
Deng, Y., Wang, S., Bai, X., Luo, G., Wu, L., Cao, Y., Li, H., Li, C., Yang, Y., Hu, Z., Tian, S., 2020. Variation trend of global soil moisture and its cause analysis. Ecol. Indic. 110, 105939.
Dorigo, W., de Jeu, R., Chung, D., Parinussa, R., Liu, Y., Wagner, W., Fernández-Prieto, D., 2012. Evaluating global trends (1988–2010) in harmonized multi-satellite surface soil moisture. Geophys. Res. Lett. 39 (18).
Feng, H., Zhang, M., 2015. Global land moisture trends: drier in dry and wetter in wet over land. Sci. Rep. 5 (1), 1–6.
GCOS, 2010. Implementation Plan for the Global Observing System for Climate (GCOS) in Support of the United Nations Framework Convention on Climate Change (UNFCCC). World Meteorological Organization, Geneva, Switzerland.
Giorgi, F., Lionello, P., 2008. Climate change projections for the Mediterranean region. Glob. Planet. Chang. 63 (2–3), 90–104.
González-Zamora, Á., Almendra-Martín, L., de Luis, M., Martínez-Fernández, J., 2021. Influence of soil moisture vs. climatic factors in Pinus Halepensis growth variability in Spain: a study with remote sensing and modeled data. Remote Sens. 13 (4), 757.
Grillakis, M.G., 2019. Increase in severe and extreme soil moisture droughts for Europe under climate change. Sci. Total Environ. 660, 1245–1255.
Gudmundsson, L., Seneviratne, S.I., 2015. European drought trends. Proc. Int. Assoc. Hydrol. Sci. 369, 75–79.
Hamed, K.H., Rao, A.R., 1998. A modified Mann-Kendall trend test for autocorrelated data. J. Hydrol. 204 (1–4), 182–196.
Hänsel, S., Ustrnul, Z., Łupikasza, E., Skalak, P., 2019. Assessing seasonal drought variations and trends over Central Europe. Adv. Water Resour. 127, 53–75.
Hersbach, H., Bell, B., Berrisford, P., Hirahara, S., Horányi, A., Muñoz-Sabater, J., Nicolas, J., Peubey, C., Radu, R., Schepers, D., Simmons, A., Soci, C., Abdalla, S., Abellan, X., Balsamo, G., Bechtold, P., Biavati, G., Bidlot, J., Bonavita, M., De Chiara, G., Dahlgren, P., Dee, D., Diamantakis, M., Dragani, R., Flemming, J., Forbes, R., Fuentes, M., Geer, A., Haimberger, L., Healy, S., Hogan, R.J., Hólm, E., Janisková, M., Keeley, S., Laloyaux, P., Lopez, P., Lupu, C., Radnoti, G., de

Rosnay, P., Rozum, I., Vamborg, F., Villaume, S., Thépaut, J.N., 2020. The ERA5 global reanalysis. Q. J. R. Meteorol. Soc. 146 (730), 1999–2049.
Huang, N.E., Shen, Z., Long, S.R., Wu, M.C., Shih, H.H., Zheng, Q., Yen, N.C., Tung, C.C., Liu, H.H., 1998. The empirical mode decomposition and the Hilbert spectrum for nonlinear and non-stationary time series analysis. Proc. R. Soc. Lon. Ser. A – Math. Phys. Eng. Sci. 454 (1971), 903–995.
Hynčica, M., Huth, R., 2019. Long-term changes in precipitation phase in Europe in cold half year. Atmos. Res. 227, 79–88.
Jaagus, J., Aasa, A., Aniskevich, S., Boincean, B., Bojariu, R., Briede, A., Danilovich, I., Dominguez-Castro, F., Dumitrescu, A., Labuda, M., Labudová, L., Lõhmus, K., Melnik, V., Mõisja, K., Pongracz, R., Potopová, V., Řezníčková, L., Rimkus, Semenova I., Stonevičius, E., Štěpánek, P., Trnka, M., Vicente-Serrano, S., Wibig, J., Zahradníček, P., 2021. Long-term changes in drought indices in eastern and central Europe. Int. J. Climatol. 42 (1), 225–249.
Kendall, M.G., 1948. Rank Correlation Methods. Griffin, London, UK.
Kramer, P.J., 1944. Soil moisture in relation to plant growth. Bot. Rev. 10 (9), 525–559.
Laguardia, G., Niemeyer, S., 2008. On the comparison between the LISFLOOD modelled and the ERS/SCAT derived soil moisture estimates. Hydrol. Earth Syst. Sci. 12 (6), 1339–1351.
Lee, T., Ouarda, T.B., 2011. Prediction of climate nonstationary oscillation processes with empirical mode decomposition. J. Geophys. Res. Atmos. 116 (D6).
Li, X., Gao, X., Wang, J., Guo, H., 2015. Microwave soil moisture dynamics and response to climate change in Central Asia and Xinjiang Province, China, over the last 30 years. J. Appl. Remote. Sens. 9 (1), 096012.
Li, M., Wu, P., Ma, Z., 2020. A comprehensive evaluation of soil moisture and soil temperature from third-generation atmospheric and land reanalysis data sets. Int. J. Climatol. 40 (13), 5744–5766.
Mann, H.B., 1945. Nonparametric tests against trend. Econometrica 13, 245–259.
Martínez-Fernández, J., González-Zamora, A., Sánchez, N., Gumuzzio, A., 2015. A soil water based index as a suitable agricultural drought indicator. J. Hydrol. 522, 265–273.
Martínez-Fernández, J., González-Zamora, A., Almendra-Martín, L., 2021. Soil moisture memory and soil properties: an analysis with the stored precipitation fraction. J. Hydrol. 593, 125622.
Masseroni, D., Camici, S., Cislaghi, A., Vacchiano, G., Massari, C., Brocca, L., 2021. The 63-year changes in annual streamflow volumes across Europe with a focus on the Mediterranean basin. Hydrol. Earth Syst. Sci. 25 (10), 5589–5601.
Merchant, C.J., Embury, O., Roberts-Jones, J., Fiedler, E., Bulgin, C.E., Corlett, G.K., Good, S., McLaren, A., Rayner, N., Morak-Bozzo, S., Donlon, C., 2014. Sea surface temperature datasets for climate applications from phase 1 of the European Space Agency Climate Change Initiative (SST CCI). Geosci. Data J. 1 (2), 179–191.
Merz, B., Plate, E.J., 1997. An analysis of the effects of spatial variability of soil and soil moisture on runoff. Water Resour. Res. 33 (12), 2909–2922.
Muñoz-Sabater, J., Dutra, E., Agustí-Panareda, A., Albergel, C., Arduini, G., Balsamo, G., Boussetta, S., Choulga, M., Harrigan, S., Hersbach, H., Martens, B., Miralles, D.G., Piles, M., Rodríguez-Fernández, N.J., Zsoter, E., Buontempo, C., Thépaut, J.N., 2021. ERA5-Land: a state-of-the-art global reanalysis dataset for land applications. Earth Syst. Sci. Data Discuss. 1–50.
Narayanankutty, K.A., Nair, A., Soori, D., Pradeep, D., Teja, V.R., KB, V., 2010. Cognitive radio sensing using hilbert huang transform. Wirel. Eng. Technol. 1, 36–40.
Naumann, G., Cammalleri, C., Mentaschi, L., Feyen, L., 2021. Increased economic drought impacts in Europe with anthropogenic warming. Nat. Clim. Chang. 11 (6), 485–491.
Pan, N., Wang, S., Liu, Y., Zhao, W., Fu, B., 2019. Global surface soil moisture dynamics in 1979–2016 observed from ESA CCI SM dataset. Water 11 (5), 883.
Peel, M.C., Finlayson, B.L., McMahon, T.A., 2007. Updated world map of the Köppen-Geiger climate classification. Hydrol. Earth Syst. Sci. 11 (5), 1633–1644.
Piles, M., Ballabrera-Poy, J., Muñoz-Sabater, J., 2019. Dominant features of global surface soil moisture variability observed by the SMOS satellite. Remote Sens. 11 (1), 95.
Piles, M., Muñoz-Marí, J., Guerrero-Curieses, A., Camps-Valls, G., Rojo-Álvarez, J.L., 2021. Autocorrelation metrics to estimate soil moisture persistence from satellite time series: application to semiarid regions. IEEE Trans. Geosci. Remote Sens. 60, 1–17.
Preimesberger, W., Scanlon, T., Su, C.H., Gruber, A., Dorigo, W., 2020. Homogenization of structural breaks in the global ESA CCI soil moisture multisatellite climate data record. IEEE Trans. Geosci. Remote Sens. 59 (4), 2845–2862.
Qiu, J., Gao, Q., Wang, S., Su, Z., 2016. Comparison of temporal trends from multiple soil moisture data sets and precipitation: the implication of irrigation on regional soil moisture trend. Int. J. Appl. Earth Obs. Geoinf. 48, 17–27.
Rahmani, A., Golian, S., Brocca, L., 2016. Multiyear monitoring of soil moisture over Iran through satellite and reanalysis soil moisture products. Int. J. Appl. Earth Obs. Geoinf. 48, 85–95.
Sang, Y.F., Wang, Z., Liu, C., 2013. Discrete wavelet-based trend identification in hydrologic time series. Hydrol. Process. 27 (14), 2021–2031.
Sang, Y.F., Wang, Z., Liu, C., 2014. Comparison of the MK test and EMD method for trend identification in hydrological time series. J. Hydrol. 510, 293–298.
Sang, Y.F., Sun, F., Singh, V.P., Xie, P., Sun, J., 2018. A discrete wavelet spectrum approach for identifying non-monotonic trends in hydroclimate data. Hydrol. Earth Syst. Sci. 22 (1), 757–766.
Sang, Y.F., Sivakumar, B., Zhu, Y., 2021. Uniform discrete wavelet spectrum for detection of hydrologic variability at multiple timescales. J. Hydro-Environ. Res. 35, 31–37.
Seneviratne, S.I., Corti, T., Davin, E.L., Hirschi, M., Jaeger, E.B., Lehner, I., Orlowsky, B., Teuling, A.J., 2010. Investigating soil moisture–climate interactions in a changing climate: a review. Earth Sci. Rev. 99 (3–4), 125–161.
Sheffield, J., Wood, E.F., 2007. Characteristics of global and regional drought, 1950–2000: analysis of soil moisture data from off-line simulation of the terrestrial hydrologic cycle. J. Geophys. Res. Atmos. 112 (D17).
Sheffield, J., Wood, E.F., 2008. Global trends and variability in soil moisture and drought characteristics, 1950–2000, from observation-driven simulations of the terrestrial hydrologic cycle. J. Clim. 21 (3), 432–458.
Siebert, S., Döll, P., Hoogeveen, J., Faures, J.M., Frenken, K., Feick, S., 2005. Development and validation of the global map of irrigation areas. Hydrol. Earth Syst. Sci. 9 (5), 535–547.
Smith, P.J., Pappenberger, F., Wetterhall, F., Del Pozo, J.T., Krzeminski, B., Salamon, P., Muraro, D., Kalas, M., Baugh, C., 2016. On the operational implementation of the European Flood Awareness System (EFAS). Flood Forecasting. Academic Press, pp. 313–348.
Song, X., Song, Y., Chen, Y., 2020. Secular trend of global drought since 1950. Environ. Res. Lett. 15 (9), 094073.
Spinoni, J., Vogt, J.V., Naumann, G., Barbosa, P., Dosio, A., 2018. Will drought events become more frequent and severe in Europe? Int. J. Climatol. 38 (4), 1718–1736.
Trenberth, K.E., 2011. Changes in precipitation with climate change. Clim. Res. 47 (1–2), 123–138.
Trnka, M., Dubrovský, M., Svoboda, M., Semerádová, D., Hayes, M., Žalud, Z., Wilhite, D., 2008. Developing a regional drought climatology for the Czech Republic. Int. J. Climatol. 29 (6), 863–883.
Trnka, M., Kyselý, J., Možný, M., Dubrovský, M., 2009. Changes in Central-European soil-moisture availability and circulation patterns in 1881–2005. Int. J. Climatol. 29 (5), 655–672.
Van Der Knijff, J.M., Younis, J., De Roo, A.P.J., 2010. LISFLOOD: a GIS-based distributed model for river basin scale water balance and flood simulation. Int. J. Geogr. Inf. Sci. 24 (2), 189–212.
Vautard, R., Yiou, P., D'andrea, F., De Noblet, N., Viovy, N., Cassou, C., Polcher, J., Ciais, P., Kageyama, M., Fan, Y., 2007. Summertime European heat and drought waves induced by wintertime Mediterranean rainfall deficit. Geophys. Res. Lett. 34 (7).
Vicente-Serrano, S.M., Domínguez-Castro, F., Murphy, C., Hannaford, J., Reig, F., Peña-Angulo, D., Tramblay, Y., Trigo, R.M., Mac Donald, N., Luna, M.Y., Mc Carthy, M., Van der Schrier, G., Turco, M., Camuffo, D., Noguera, I., García-Herrera, R., Becherini, F., Della Valle, A., Tomas-Burguera, M., El Kenawy, A., 2021. Long-term variability and trends in meteorological droughts in Western Europe (1851–2018). Int. J. Climatol. 41, E690–E717.
Wei, F., Wang, S., Fu, B., Pan, N., Feng, X., Zhao, W., Wang, C., 2018. Vegetation dynamic trends and the main drivers detected using the ensemble empirical mode decomposition method in East Africa. Land Degrad. Dev. 29 (8), 2542–2553.
Wu, Z., Huang, N.E., 2004. A study of the characteristics of white noise using the empirical mode decomposition method. Proc. R. Soc. Lon. Ser. A – Math. Phys. Eng. Sci. 460 (2046), 1597–1611.
Wu, Z., Huang, N.E., 2005. Statistical significance test of intrinsic mode functions. In: Hilbert-Huang Transform and its Applications. World Sci, Singapore, pp. 107–127.
Wu, Z., Huang, N.E., 2009. Ensemble empirical mode decomposition: a noise-assisted data analysis method. Adv. Adapt. Data Anal. 1 (01), 1–41.
Zawadzki, J., Kędzior, M., 2014. Statistical analysis of soil moisture content changes in Central Europe using GLDAS database over three past decades. Open Geosci. 6 (3), 344–353.
Zhang, R., Li, L., Zhang, Y., Huang, F., Li, J., Liu, W., Mao, T., Xiong, Z., Shangguan, W., 2021. Assessment of agricultural drought using soil water deficit index based on ERA5-land soil moisture data in four Southern provinces of China. Agriculture 11 (5), 411.